Translational Oncology
www.transonc.com

Volume 11 Number xx Month 2018 pp. 56–64 56

Predicting Treatment Response of Breast Cancer to Neoadjuvant Chemotherapy Using Ultrasound-Guided Diffuse Optical Tomography

Wenxiang Zhi[*], Guangyu Liu[†], Cai Chang[*], Aiyu Miao[*], Xiaoli Zhu[‡], Li Xie[§] and Jin Zhou[*]

[*]Department of Ultrasonography, Fudan University, Shanghai Cancer Center, Department of Oncology, Shanghai Medical College, Fudan University, No 270, Dong'an Road, Xuhui District, Shanghai, 200032, China; [†]Department of Breast Surgery, Fudan University, Shanghai Cancer Center, Department of Oncology, Shanghai Medical College, Fudan University, No 270, Dong'an Road, Xuhui District, Shanghai, 200032, China; [‡]Department of Pathology, Fudan University, Shanghai Cancer Center, Department of Oncology, Shanghai Medical College, Fudan University, No 270, Dong'an Road, Xuhui District, Shanghai, 200032, China; [§]Clinical Statistics Center, Fudan University Shanghai Cancer Center, Department of Oncology, Shanghai Medical College, Fudan University, No 270, Dong'an Road, Xuhui District, Shanghai, 200032, China

Abstract

PURPOSE: To prospectively investigate ultrasound-guided diffuse optical tomography (US-guided DOT) in predicting breast cancer response to neoadjuvant chemotherapy (NAC). *MATERIALS AND METHODS:* Eighty-eight breast cancer patients, with a total of 93 lesions, were included in our study. Pre– and post–last chemotherapy, size and total hemoglobin concentration (THC) of each lesion were measured by conventional US and US-guided DOT 1 day before biopsy (time point t0, THC THC0, SIZE S0) and 1 to 2 days before surgery (time point tL, THCL, SL). The relative changes in THC and SIZE of lesions after the first and last NAC cycles were considered as the variables ΔTHC and ΔSIZE. Receiver operating characteristic curve was performed to calculate ΔTHC and ΔSIZE cutoff values to evaluate pathologic response of 93 breast cancers to NAC, which were then prospectively used to predicate response of 61 breast cancers to NAC. *RESULTS:* The cutoff values of ΔTHC and ΔSIZE for evaluation of breast cancers NAC treatment response were 23.9% and 42.6%. At ΔTHC 23.9%, the predicted treatment response in 61 breast lesions for the time points t1 to t3 was calculated by area under the curve (AUC), which were AUC_1 0.534 ($P = .6668$), AUC_2 0.604 ($P = .1893$), and AUC_3 0.674($P =$. 0.027), respectively; for ΔSIZE 42.6%, at time points t1 to t3, AUC_1 0.505 ($P = .9121$), AUC_2 0.645 ($P = .0115$), and AUC_3 0.719 ($P = .0018$). *CONCLUSION:* US-guided DOT ΔTHC 23.9% and US ΔSIZE 42.6% can be used for the response evaluation and earlier prediction of the pathological response after three rounds of chemotherapy.

Translational Oncology (2018) 11, 56–64

Introduction

In females, breast cancer is the most common cancer that causes major cancer mortality [1]. Neoadjuvant chemotherapy (NAC) has become the standard treatment for locally advanced breast cancer. NAC can downstage breast cancer, inhibit micrometastases, improve breast-conserving therapeutic strategy during surgery, and assess preoperative lesion sensitivity to medication [2]. Complete eradica-

Address all correspondence to: Cai Chang, Department of Ultrasonography, Fudan University Shanghai Cancer Center, Department of Oncology, Shanghai Medical College, Fudan University, No. 270 Dong'an road, Shanghai 200032, China.
E-mail: changc61@163.com
Received 24 September 2017; Revised 26 October 2017; Accepted 30 October 2017

1936-5233
https://doi.org/10.1016/j.tranon.2017.10.011

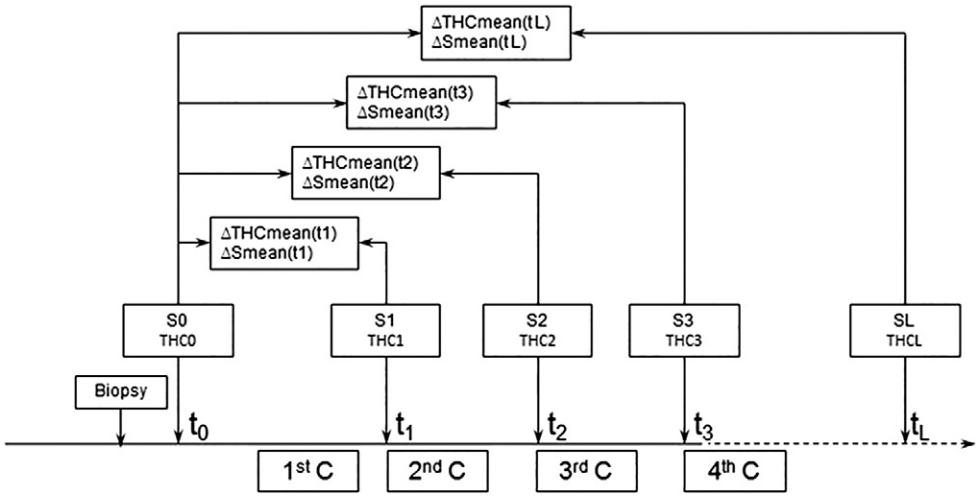

Figure 1. The flowchart of the study design with the THC and SIZE parameters derived from US and US-guided DOT images at four time points of the NAC rounds. *C*, cycle.

tion of invasive tumor cells in primary tumor bed following NAC renders longer disease-free survival [3,4]. Preoperative assessment of breast cancer NAC response is crucial since it helps physicians to decide the deadline of chemotherapy regimens. Conventional mammography, ultrasound [5], and magnetic resonance imaging (MRI) [6], which are based on tumor size changes, have been reported to assess response. Functional imaging techniques, such as dynamic contrast-enhanced (CE-MRI), MR spectroscopy, and positron emission tomography (PET) [7–9], have been used to monitor cancer response to NAC and demonstrated promising initial results. But mammography with radiation, PET, and CE-MRI, involving costly facilities and inserting drugs invasively, are not very desirable imaging modalities.

Diffuse optical tomography (DOT) is an optical imaging technique that uses near-infrared light to probe the absorption and scattering properties of biologic tissues and to acquire information of tumor physiology, biochemistry, angiogenesis, and hypoxia [10–13]. Because of the poor spatial resolution caused by intense light scattering in soft tissue, DOT alone has not been widely used in clinical studies. DOT combined with other imaging techniques such as x-ray mammography, MRI, or ultrasonography (US) for lesion locating has been explored for breast cancer diagnosis and monitoring NAC responses for locally advanced breast cancers [14–16]. Presurgical evaluation of NAC efficacy in solid tumors has been solely reliant on anatomical tumor burden and its alteration [17]. Given the long duration of NAC and poor patient compliance, so far, all the studies on US-guided DOT evaluation of breast cancer NAC efficacy had been limited to very small sample pools (10-34 patients) [10,18–26], without referring to ΔTHC best cutoff values to assess pathologic response. Therefore, our current study assembled a much larger cohort to investigate the best cutoff values to differentiate NAC responder group from nonresponder group and time points to get maximum diagnostic performance, as well as early predictive value of US-guided DOT ΔTHC in evaluating breast cancer pathologic response to NAC.

Materials and Methods

Study Design and Population

Patients were recruited from Fudan University Shanghai Cancer Center (FUSCC) from September 2014 to May 2016. The study protocol was approved by the institutional review board of the Human Subjects Protection Office of FUSCC. Written informed consent was obtained from all patients. FUSCC is one of the largest cancer centers in China with approximately 4500 breast cancer patients receiving surgical resection treatment in the past 2 years.

All study subjects were pathologically diagnosed before receiving neoadjuvant treatment. Patients received four to eight rounds of NAC according to their molecular subtypes.

One hundred and seventy-eight lesions in 170 female patients were included in presurgical NAC, 85 lesions later were excluded: 79 did not have the last US-guided DOT evaluation at the end of presurgery NAC; 4 lesions were located too shallow, only 1 to 2 mm away from the skin; 2 lesions were located close to nipples, showing nipple artifacts. In all, 93 lesions with pre– and post–last chemotherapy (mean size, 41 mm; range, 14 to 93 mm) in 88 patients (mean age, 50 years; range, 32 to 82 years) were included in the final data analysis. Because, according to RECIST guidelines [27], all baseline evaluations should be performed as close as possible to the beginning of treatment, US-guided DOT evaluation was done within a week of starting NAC.

Pre– (time point t0) and post–last (time point tL) chemotherapy, the size and total hemoglobin concentration (THC) of each lesion were measured by conventional US and US-guided DOT 1 day before biopsy (time point t0, THC0, S0) and 1 to 2 days before surgery (time point tL THCL, SL). The relative changes in THC and SIZE of lesions after the first and last NAC rounds were considered as the variables ΔTHC and ΔSIZE. The area under the ROC curve (AUC) was used to calculate the cutoff values of ΔTHC and ΔSIZE in predicting pathologic responses and was prospectively tested in 61 breast lesions which were measured using both US and US-guided DOT (time point t0-t3, tL, THC0-THC3, THCL, S0-S3, SL). THC and SIZE of 61 breast lesions were measured by conventional US and US-guided DOT 1 day before biopsy (time point t0, THC0, S0), 1 day before next NAC cycle (time point t1-t3, THC1-THC3, S1-S3), and 1 day before surgery (time point tL, THCL,SL) (Figure 1).The NAC clinical efficacy was determined with surgical pathologic examination results as the verification standard.

Ultrasonography and US-Guided DOT Acquisition and Evaluation Criterion of 93 Target Lesions Response

The US examinations were performed using the Aixplorer US system (SuperSonic Imagine, Aix-en-Provence, France) with a SL15-4 multifrequency linear probe operating at 4 to 15 MHz. The breast

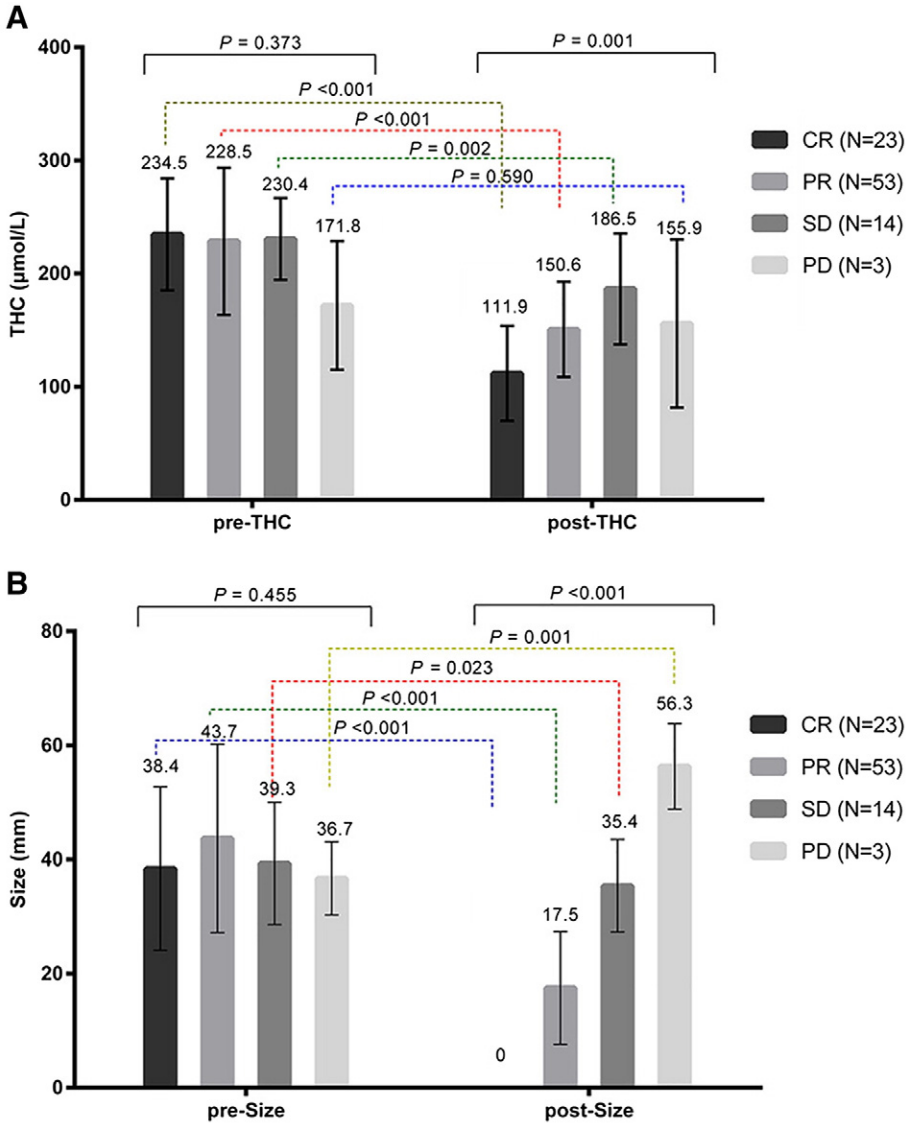

Figure 2. Pre- and post-NAC parameters changes of CR, PR, SD, and PD groups. (A) Pre- and post-NAC THC of CR, PR, SD, and PD groups. (B) Pre- and post-NAC tumor size of CR, PR, SD, and PD groups.

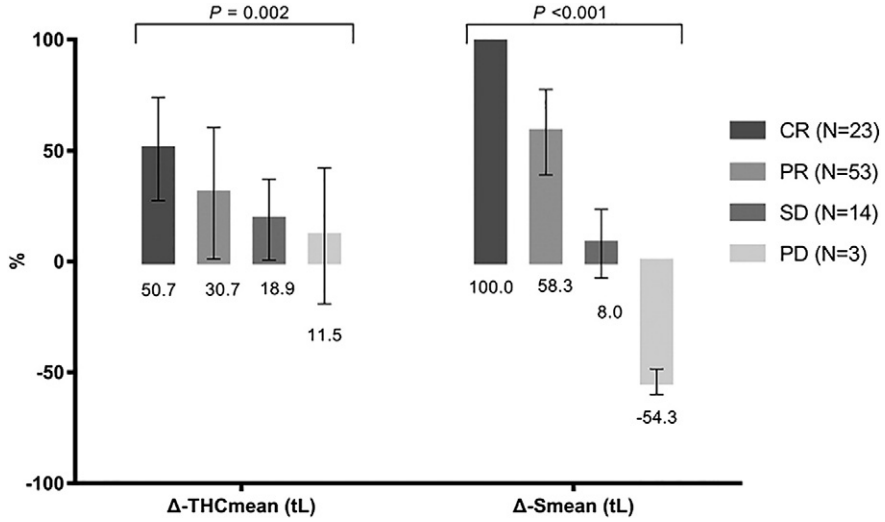

Figure 3. Pre- and post-NAC ΔSmean (tL) and ΔTHCmean (tL) of CR, PR, SD, and PD groups.

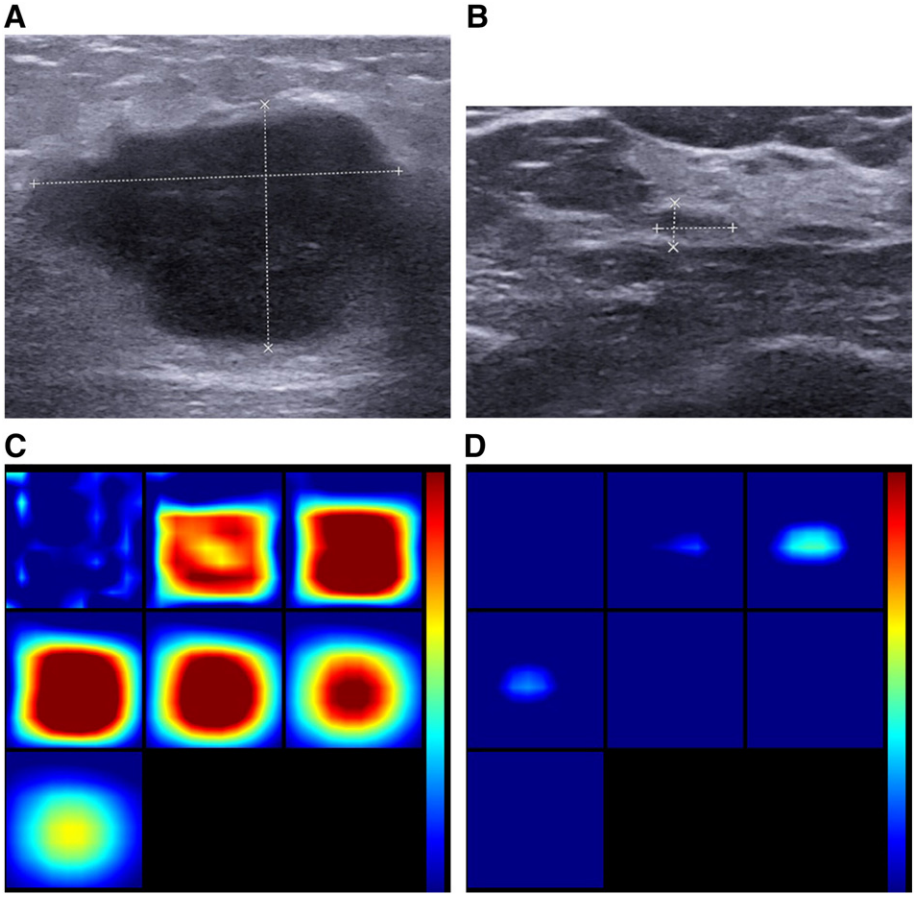

Figure 4. One responder case: invasive ductal carcinoma in a 48-year-old woman. (A, B) US images show a pre- and posttreatment lesion with hypoechoic, irregular shape and indistinct margins, with US measuring pre-size of 3.6 cm and post-size 0.7 cm in diameter. It was a pathologically complete response with Miller-Payne grade 5; therefore, ΔSmean (tL) was 100%. (C, D) Pre- and posttreatment reconstructed optical absorption maps show that the lesion was resolved in slices from 1 (top left, left to right) to 7 (bottom left, left to right) and from 2 to 4 (top row, left to right). Pre- and posttreatment THCs were 279.0 μmol/L and 128.0 μmol/L, respectively. ΔTHCmean (tL) of the lesion was 54.1%. The first section (slice 1, top left) is a 6 × 6–cm spatial *x-y* image (coronal plane of the body) obtained at a depth of 0.5 cm, as measured from the skin surface. The last section (slice 7, bottom left) is a 6 × 6–cm spatial *x-y* image (coronal plane of the body) obtained at a depth of 3.5 cm towards the chest wall. Spacing between sections is 0.5 cm in the direction of propagation. The vertical color scale from blue to red is the THC in micromoles per liter from low to high.

US examinations were performed by the same radiologists (W.X.Z. and A.Y.M. with more than 9 years of experience in breast US) according to the American Institute of Ultrasound in Medicine practice guidelines for performing breast US [28], with the patient in the supine position. The US respectively measured pre- and post-NAC lesion sizes (t1and tL, S0 and SL) (maximal diameters) of 93 lesions. The relative change in size after the first and last NAC cycles was considered as the variable ΔSize(tL). ΔSize(tL) = (S0 – SL)/S0 × 100%. Based on the Guidelines to Evaluate the Response to Treatment in Solid Tumors [27], the responses to NAC were classified into complete response (CR), partial response (PR), static disease (SD), progressive disease (PD) groups. Patients with CR and PR were assigned as responders, and patients with SD and PD as nonresponders on conventional US [7].

US-guided DOT, using Optimus-01HWS breast diagnostic system (XinAo-MDT Technology, Hebei, China), which is a dual imaging modality combining conventional ultrasound (Terason T3000 ultrasound, Teratech, USA) and near-infrared (NIR) optical tomography, was used to measure functional tissue properties with optical spectroscopic analysis, The main functional parameter was the total hemoglobin concentration (THC) calculated from absorption coefficients measured by using two optical wavelengths (785 nm and 830 nm). The technical details of this imaging system, including system configurations, imaging acquisition methods, and the data processing algorithms, have been previously described by us [15]. Tumors were located by conventional US, and optical imaging was then performed using a handheld probe. After freezing the frame at the maximal section, raw optic data acquisition was performed five times for each breast lesion and the corresponding normal area in the contralateral breast. The final data were obtained by automatically or manually defining the region of interest (ROI), imaging and data computing, a process that takes about 3 to 5 minutes. The data were input into Excel files, and mean values of THC (THCmean) were established.

Therefore, each optical parameter value reported is a mean of approximately 5 values of the ROI, and the SD is a reflection of the physiologic variation for that patient. ROI was drawn to include the maximal dimension of the lesion based on the US images, which encompassed the whole area of the identified lesion and a small

Table 1. Diagnostic Performance of ΔTHCmean 23.9% and ΔSmean 42.6% in Assessing Treatment Response of 93 Breast Cancers to NAC

Variables	Sen (%)	Spe (%)	PPV (%)	NPV (%)	Accuracy (%)	AUC (95% CI)	*P* Value
ΔTHC 23.9%	73.7	76.5	93.3	76.5	74.2	0.751 (0.650-0.835)	<.0001
ΔSIZE 42.6%	80.3	52.9	88.4	37.5	77.4	0.690 (0.586-0.782)	.0125

Sen, sensitivity; *Spe*, specificity.

portion of the surrounding normal tissues. The optical imaging–measured normal site in the symmetrical region of the contralateral breast was used as references in the reconstruction. The only one optical characteristic parameter THC used in our study was related to tissue microstructure and biochemical composition such as oxygenated hemoglobin (HbO2), deoxygenated hemoglobin (Hb), and total hemoglobin concentration ([THC] = [Hb] + [HbO2]), which were obtained by calculating the difference between the lesion and the symmetric normal site. The relative change in THC after the first and last NAC cycles was considered as the variable ΔTHC. ΔTHCmean (tL) = (THCmeant0 − THCmeantL)/THCmeant0 × 100%. All examinations were performed by the same radiologist who also participated in the acquisition of conventional US images. According to RECIST1.1 guidelines [17], CR or PR is needed to deem either one the best overall response. Overall response rate (ORR) = (CR + PR)/(CR + PR + SD + PD) × 100%. Receiver operating curve (ROC) analysis was performed to analyze the diagnostic performance of ΔTHC(tL) and ΔSIZE(tL) to predict the pathological response. The best cutoff values of ΔTHC and ΔSIZE were then used to calculate the sensitivity, specificity, positive predictive value (PPV), negative predictive value (NPV), and accuracy for predicting pathological responsiveness. The NAC clinical efficacy was determined with surgical pathologic examination results as the verification standard.

Ultrasonography and US-Guided DOT Acquisition and Evaluation Criterion of 61 Target Lesions Response

We applied the predictive cutoff values of ΔTHC and ΔSIZE to 61 NAC breast lesions. In order to assess the early predictive values of ΔTHC and ΔSIZE, we analyzed breast lesions which went through top three rounds of chemotherapy. THC and SIZE of 61 breast lesions were measured by conventional US and US-guided DOT 1 day before biopsy (time point t0, THC0, S0), 1 day before next NAC cycle (time point t1-t3,THC1-THC3, S1-S3), and 1 day before surgery (time point tL, THCL,SL) (Figure 1). The relative changes in SIZE and THC of the primary tumor from baseline were calculated at four different time points (S1, THC1 at t1, S2, THC2 at t2,S3, THC3 at t3, SL, THCL at Tl) using the following equations:

$$\Delta\text{THCmean}(t1) = (\text{THC0mean}-\text{THC1mean})/\text{THC0mean} \times 100\%$$
$$\Delta\text{THCmean}\ (t2) = (\text{THC0mean}-\text{THC2mean})/\text{THC0mean} \times 100\%$$
$$\Delta\text{THCmean}\ (t3) = (\text{THC0mean}-\text{THC3mean})/\text{THC0mean} \times 100\%$$
$$\Delta\text{THCmean}\ (tL) = (\text{THC0mean}-\text{THCLmean})/\text{THC0mean} \times 100\%$$

$$\Delta\text{Smean}\ (t1) = (\text{S0mean}-\text{S1mean})/\text{S0mean} \times 100\%$$
$$\Delta\text{Smean}\ (t2) = (\text{S0mean}-\text{S2mean})/\text{S0mean} \times 100\%$$
$$\Delta\text{Smean}(t3) = (\text{S0mean}-\text{S3mean})/\text{S0mean} \times 100\%$$
$$\Delta\text{Smean}\ (tL) = (\text{S0mean}-\text{SLmean})/\text{S0mean} \times 100\%$$

Figure 1 illustrates the flowchart of the study design with the THC and SIZE parameters derived from US and US-guided DOT images at four time points of the NAC rounds.

Pathological Evaluation of NAC Efficacy

The final pathologic response was assessed using the Miller-Payne grading system [29], in which pathologic response is divided into five grades based on comparison of tumor cellularity between pre-NAC core biopsy and postoperative surgical specimen. For this study, two pathologists performed final diagnosis, and discrepancies were resolved by consensus. Responders were categorized as having a Miller-Payne grades 3 or 4 or 5, while nonresponders had grades 1or 2.

Statistical Analysis

Statistical analyses were performed with MedCalc software (version 15.2.2; Med-Calc, Mariakerke, Belgium). The one-way ANOVA and paired-sample *t* test were used to estimate group differences for SIZE and THC parameters of different time points, with $P < .05$ considered a statistically significant difference. With postsurgical Miller-Payne grading as the gold standard, ROC curves were used to analyze the best cutoff values of ΔTHC and ΔSize to differentiate NAC responder group from nonresponder and to predict the clinical efficacy of breast cancer NAC.

Results

Out of 93 lesions, 23 had CR, 53 PR, 14 SD, and 3 PD. Figure 2 indicated US-guided DOT monitoring pre-NAC and post-NAC parameters of different groups. As shown in Figure 2*A*, although before NAC THC had no difference among the groups ($F = 1.053$, $P = .373$), after NAC treatment, THC varied significantly ($F = 5.80$, $P = .001$), with the lowest THC reading in CR group, higher in PD and SD groups. Within each group, except for group PD ($P = .590$), THC changed significantly: CR ($P < .001$), PR ($P < .001$), SD ($P = .002$). As demonstrated in Figure 2*B*, pretreatment tumor sizes were similar among the groups ($F = 2.617$, $P = .455$); post-NAC tumors sizes were significantly different ($F = 69.77$, $P < .001$): tumors size of CR was 0 and gradually increased in PR, SD, and PD groups. Not surprisingly, pre- and post-NAC tumor sizes were significantly different in all groups: CR ($P < .001$), PR ($P < .001$), SD ($P = .023$), PD ($P = .001$). Figure 3 illustrated that ΔSmean (tL) ($F = 150.9$, $P < .001$) and ΔTHCmean (tL) ($F = 5.43$, $P = .002$) differed significantly among the groups: ΔSmean (tL) was highest in group CR (100%) (Figure 4): PR 58.3 ± 19.2%, SD 8.0 ± 015.6%, PD −54.3 ± 5.7%; ΔTHCmean (tL) was also highest in CR group (Figure 4): 50.7 ± 23.2%, PR 30.7 ± 29.6%, SD 18.9 ± 18.3%, PD −11.5 ± 30.7%.

Table 2. Diagnostic Performance of ΔTHC 23.9% and ΔSIZE 42.6% in Predicting 61 Breast Cancers Lesions' Response to NAC at Different Cycles

Parameters at Different Time Points	Sen	Spe	PPV	NPV	Accuracy	AUC (95% CI)	*P* Value
ΔTHCmean (t1)	0.34	0.727	0.850	0.195	0.410	0.534(0.401-0.663)	.6668
ΔTHCmean (t2)	0.48	0.727	0.889	0.235	0.525	0.604(0.470-0.727)	.1893
ΔTHCmean (t3)	0.62	0.727	0.912	0.296	0.639	0.674(0.542-0.788)	.0270
ΔTHCmean (tL)	0.70	0.727	0.921	0.348	0.705	0.714(0.584-0.822)	.0059
ΔSIZEmean (t1)	0.08	0.909	0.800	0.179	0.230	0.505(0.374-0.636)	.9121
ΔSIZEmean (t2)	0.38	0.909	0.950	0.244	0.475	0.645(0.512-0.763)	.0115
ΔSIZEmean (t3)	0.62	0.818	0.939	0.321	0.656	0.719(0.589-0.827)	.0018
ΔSIZEmean (tL)	0.86	0.455	0.878	0.417	0.787	0.657(0.525-0.774)	.0567

Of the 93 breast cancer lesions, according to the RECIST 1.1 criteria, 76 breast cancers were responders, and 17 breast cancers were non-responders, ORR 为81.7%. ROC curve analysis was used to identify maximum value sum of sensitivity and specificity, while ΔTHCmean 23.9% and ΔSmean 42.6% were used as the threshold value to differentiate NAC responder group from nonresponder group. The sensitivity, specificity, PPV, NPV, and accuracy of US-guided DOT were 73.7%, 76.5%, 93.3%, 76.5%, and 74.2%, respectively. The AUC was 0.751 (95% CI: 0.650-0.835). The sensitivity, specificity, PPV, NPV, and accuracy of conventional US were 80.3%, 52.9%, 88.4%, 37.5%, and 77.4%, respectively. The AUC was 0.690 (0.586-0.782) (Table 1). We then applied the cutoff

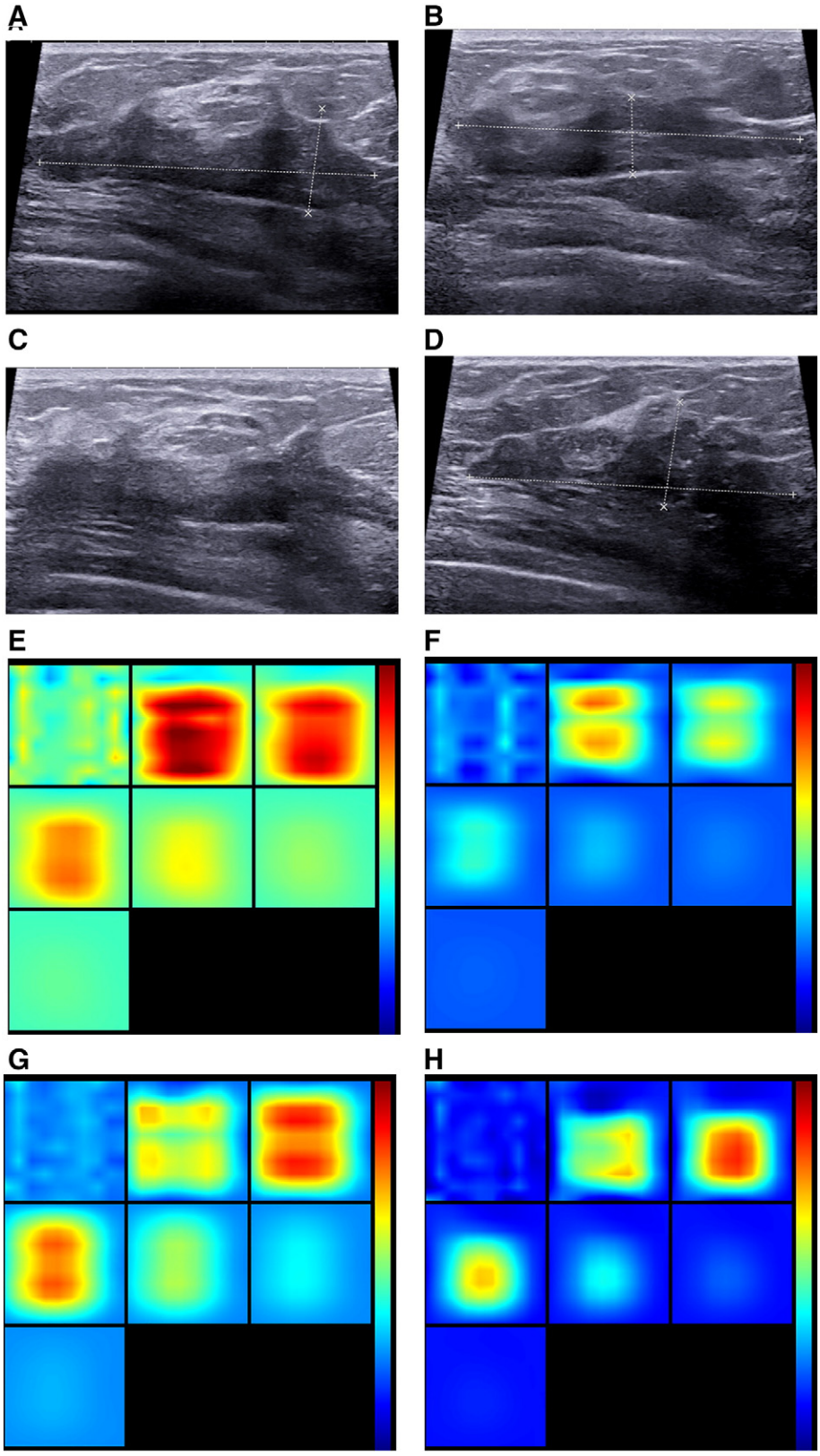

values of ΔTHCmean 23.9% and ΔSmean 42.6% to the breast lesions that went through various NAC rounds to predict pathologic responses (Table 2) (Figures 5-6). Our results showed that, at ΔSmean 42.6%, the AUCs of NAC responder group after chemotherapy rounds were: AUC_1 = 0.505 (95% CI: 0.374-0.636), P = .9121, AUC_2 = 0.645 (95% CI: 0.512-0.763), P = .0115, AUC_3 = 0.719 (95% CI: 0.589-0.827), P = .0018, and AUC_L =0.657 (95% CI: 0.525-0.774), P = .0567. The sensitivity and accuracy were climbing higher from t1 to t3. As early as after the second round of NAC, ΔSmean 42.6% was able to differentiate responder group from nonresponder group (P = .0115), with AUC reaching the highest value at t3. For ΔTHC 23.9%, the AUCs were AUC_1 = 0.534 (95% CI: 0.401-0.663), P = .6668, AUC_2 = 0.604 (95% CI: 0.470-0.727), P = .1893, AUC_3 = 0.674 (95% CI: 0.542-0.788), P = .027, and AUC_L = 0.714 (95% CI: 0.584-0.822), P = .0059. The sensitivity and accuracy showed a similar trend as the ΔSmean 42.6%. As early as after the third round of NAC, ΔTHC 23.9% could differentiate responder group from nonresponder group (P = .027).

Discussion

US-guided DOT, as functional imaging technique without use of exogenous contrast agents, is relatively inexpensive and short-timed compared to with MRI and PET [30]. This technique also provides functional information as a potential complement to traditional structural imaging techniques of MRI and conventional US. Previous studies with small sample pools have demonstrated the feasibility of using DOT for monitoring treatment in patients with locally advanced breast cancer, with diffuse optical parameters of THC to indicate angiogenesis and oxygen saturation of tumor tissue, i.e., cancer cell growth [18,20].

In our current study with more lesion samples, we found no difference of THC reading among the groups before the NAC, indicating that pretreatment THC measurements may not predict therapy efficacy. This finding is apparently different from what Zhu et al. [25] discovered in their cohort of 32 lesions. The possible reason for this discrepancy could be due to the pre-DOT needle biopsy procedures in that study, as a bruise or hematoma caused by prior biopsy may have some effect on THC measurements.

For posttreatment data, THC measurements and ΔTHC all showed significant variations among groups, with the lowest THC reading and highest ΔTHC% found in the CR group and with the SD group having the opposite; these results of ours demonstrate the potential use of ΔTHC in evaluating breast cancer efficacy. Pakalniskis et al. [31] uncovered that, for women with CR, pretreatment MVD of CD105-expressing blood vessels correlated with high THC. Comparing prechemo with postsurgery tumor vascularity, previous studies [32] concluded that decreased tumor vascularity indicates good response and increased or unchanged vascularity indicates no response at all. Hence, in agreement with previous studies, we reiterate that THC correlates with blood vessels inside tumor lesion: the more THC decreases, the less tumor blood vessel grows, and the better the therapy efficacy achieves [33]. On the other hand, as elevated levels of THC indicating efficient blood supply to tumor, this allows for better drug and nutrients delivery to cancer cells [34]. Our data revealed a significantly higher THC in almost all pretreatment groups comparing to the posttreatment ones, suggesting NAC inhibited tumor angiogenesis.

Tumor sizes and ΔSize differed significantly among different groups, which were consistent with other research reports, confirming the value of US for evaluation of NAC efficacy in treating breast cancer [5,6]. Along with shrinking tumor size and lowered THC, ΔSize and ΔTHC also bore a signature among the groups, with highest value in CR followed by PR and SD groups.

In CR and PR groups (total 93 breast cancer lesions), facilitated by pathology reports, we further used ROC curves to analyze the efficacy of ΔSmeantL and ΔTHCmeantL in predicting pathologic response to NAC. Our results indicated that the ΔSmean 42.6% (AUC 0.751) and ΔTHC 23.9% (AUC 0.690) had moderate value in determining NAC response. This finding of ours suggests that the NAC response evaluation power of US-guided DOT is similar to DCE-MRI and PET/CT, as An et al. [7] reported that the AUCs for DCE-MRI using MR-CAD analysis and PET/CT were 0.77 and 0.76. Our results from 61 lesions also pointed out that for early prediction of NAC response (after only two rounds), ΔTHC 23.9% achieved higher sensitivity and accuracy than ΔSmean 42.6%. This finding is consistent with the previous report by Cerussi et al. [21] probably due to the fact that, in the lesions, changes of functional metabolism are always earlier than those of morphology. Overall, we found that for the first three NAC rounds, in predicting pathologic response, ΔTHC 23.9% and ΔSmean 42.6% had low sensitivity and high specificity. But the sensitivity and accuracy of these tests increased with more rounds of treatment: as early as the end of the second NAC round, ΔSmean 42.6% could differentiate responder and nonresponder groups; for ΔTHC 23.9%, it was the third round. Interestingly, the sensitivity of prediction power of ΔSmean 42.6% at the end of the second round was only 38%, lower than 62% of the third round. This finding, combined with the AUC result (AUC_2 0.645 vs AUC_3 0.719), made us conclude that the best time point for ΔSmean 42.6% to predict NAC efficacy is after the third round of treatment. Another point to add is that ΔTHC 23.9% and ΔSmean 42.6% all achieved highest NPV for prediction at the third round. In conclusion, ΔSmean 42.6% and ΔTHC 23.9% can effectively predict NAC efficacy early in treatments, around the end of the third round. Rousseau et al. [35,36] described that pathologic response to breast cancer NAC could be predicted accurately by FDG PET after two

Figure 5. One nonresponder case: invasive ductal carcinoma in a 43-year-old woman. (A, B, C, D) US images show at different time points lesion with hypoechoic, irregular shape and indistinct margins, with US measuring S0 5.0 cm (A), S1 5.1 cm (B), S2 4.8 cm (C), and S3 4.8 cm (D) in diameter. The final pathological size was 4.0 cm with Miller-Payne grade 2; therefore, ΔSmean (t1) was −2%, ΔSmean (t2) 4%, and ΔSmean (t3) 4%. (E, F, G, H) Reconstructed optical absorption maps showed that the lesion was resolved in slices from 1 (top left, left to right) to 7 (bottom left, left to right). THC0mean was 206.0 μmol/L (E), THC1mean 173.3 μmol/L (F), THC2mean 185.0 μmol/L(G), and THC3mean189.3 μmol/L (H). Therefore, ΔTHCmean (t1) was 15.9%, ΔTHCmean (t2) 10.2%, and ΔTHCmean (t3) 8.1%.The first section (slice 1, top left) is a 6 × 6–cm spatial *x-y* image (coronal plane of the body) obtained at a depth of 0.5 cm, as measured from the skin surface. The last section (slice 7, bottom left) is a 6 × 6–cm spatial *x-y* image (coronal plane of the body) obtained at a depth of 3.5 cm towards the chest wall. Spacing between sections is 0.5 cm in the direction of propagation. The vertical color scale from blue to red is the THC in micromoles per liter from low to high.

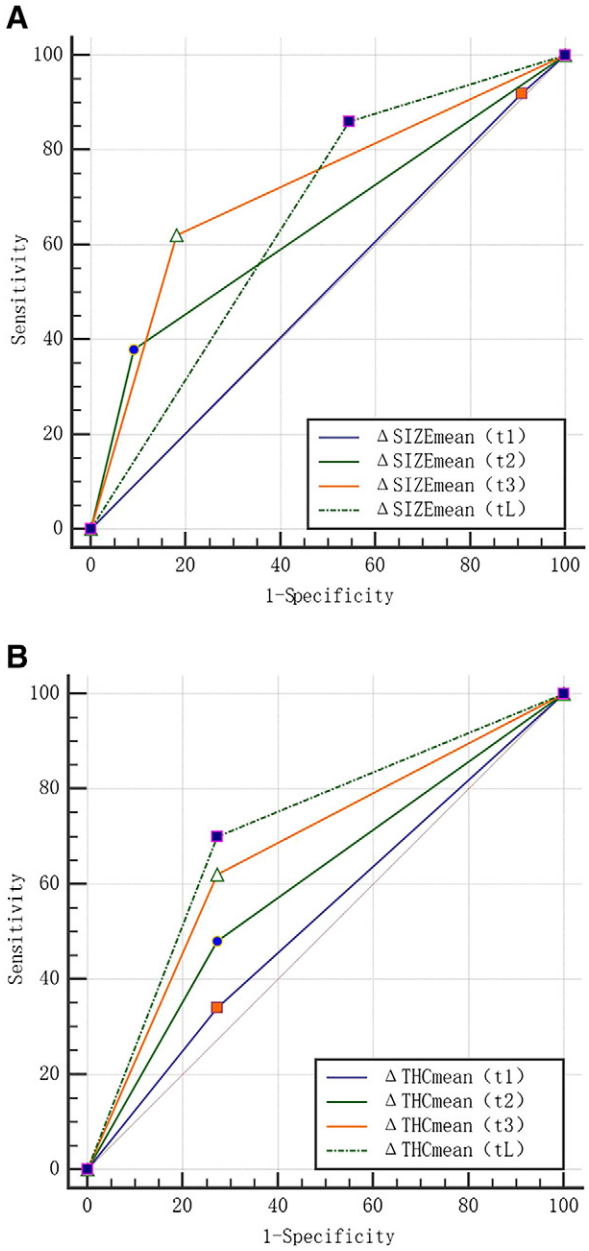

Figure 6. (A) Comparison of ΔSIZE ROC curves from the lesions treated with different chemotherapy cycles. (B) Comparison of ΔTHC ROC curves from the lesions treated with different chemotherapy cycles.

rounds of chemotherapy. Falou et al. [37] reported that Deoxygenated hemoglobin concentration and water percentage were found to be the best predictors of response at 1 week of treatment using Diffuse Optical Spectroscopy. These different optimal time points for response prediction might be a result of different imaging technologies and parameters.

Of course our study has limitations. First, the shallow lesions cannot be fully covered by the optical field due to the inherent distance between light emitter and detector in the US probe. In addition, areolar and periareolar skin has different optic absorbance, which can cause data inaccuracy. Therefore, we had to exclude all the shallow lesions (within 3 mm to the skin) as well as subareolar lesions. Secondly, we used contralateral healthy breast as normal control; lesions from one-breast patients who lost the other breast due to cancer were also excluded.

Conclusion

In summary, US-guided DOT ΔTHC 23.9% and US ΔSIZE 42.6% can be used for the response evaluation and earlier prediction of the pathological response after three rounds of chemotherapy.

Conflicts of Interest

None.

Grant Support

This work was supported by National Science Foundation of China (grant no. 81371575), National Major Scientific Research Equipment Development Project (grant no. 81627804), and Shanghai Municipal Health and Family Planning Commission (grant no. 201440424).

Acknowledgements

We appreciate the physicians of Breast Surgery and Ultrasound Departments of FUSCC for their helpful assistance with case acquisition.

References

[1] Jemal A, Bray F, Center MM, Ferlay J, Ward E, and Forman D (2011). Global cancer statistics. *CA Cancer J Clin* **61**, 69–90. https://doi.org/10.3322/caac.20107.

[2] Mauri D, Pavlidis N, and Ioannidis JP (2005). Neoadjuvant versus adjuvant systemic treatment in breast cancer: a meta-analysis. *J Natl Cancer Inst* **97**, 188–194. https://doi.org/10.1093/jnci/dji021.

[3] Wolmark N, Wang J, Mamounas E, Bryant J, and Fisher B (2001). Preoperative chemotherapy in patients with operable breast cancer: nine-year results from National Surgical Adjuvant Breast and Bowel Project B-18. *J Natl Cancer Inst Monogr* , 96–102 [PMID: 11773300].

[4] Rastogi P, Anderson SJ, Bear HD, Geyer CE, Kahlenberg MS, Robidoux A, Margolese RG, Hoehn JL, Vogel VG, Dakhil SR, et al (2008). Preoperative chemotherapy: updates of National Surgical Adjuvant Breast and Bowel Project Protocols B-18 and B-27. *J Clin Oncol* **26**, 778–785.

[5] Vriens BE, de Vries B, Lobbes MB, van Gastel SM, van den Berkmortel FW, Smilde TJ, van Warmerdam LJ, de Boer M, van Spronsen DJ, Smidt ML, et al (2016). Ultrasound is at least as good as magnetic resonance imaging in predicting tumour size post-neoadjuvant chemotherapy in breast cancer. *Eur J Cancer* **52**, 67–76.

[6] Lee MC, Gonzalez SJ, Lin H, Zhao X, Kiluk JV, Laronga C, and Mooney B (2015). Prospective trial of breast MRI versus 2D and 3D ultrasound for evaluation of response to neoadjuvant chemotherapy. *Ann Surg Oncol* **22**, 2888–2894.

[7] An YY, Kim SH, Kang BJ, and Lee AW (2015). Treatment response evaluation of breast cancer after neoadjuvant chemotherapy and usefulness of the imaging parameters of MRI and PET/CT. *J Korean Med Sci* **30**, 808–815. https://doi.org/10.3346/jkms.2015.30.6.808.

[8] Lim I, Noh WC, Park J, Park JA, Kim HA, Kim EK, Park KW, Lee SS, You EY, Kim KM, et al (2014). The combination of FDG PET and dynamic contrast-enhanced MRI improves the prediction of disease-free survival in patients with advanced breast cancer after the first cycle of neoadjuvant chemotherapy. *Eur J Nucl Med Mol Imaging* **41**, 1852–1860.

[9] Teruel JR, Heldahl MG, Goa PE, Pickles M, Lundgren S, Bathen TF, and Gibbs P (2014). Dynamic contrast-enhanced MRI texture analysis for pretreatment prediction of clinical and pathological response to neoadjuvant chemotherapy in patients with locally advanced breast cancer. *NMR Biomed* **27**, 887–896.

[10] Tromberg BJ, Cerussi A, Shah N, Compton M, Durkin A, Hsiang D, Butler J, and Mehta R (2005). Imaging in breast cancer: diffuse optics in breast cancer: detecting tumors in pre-menopausal women and monitoring neoadjuvant chemotherapy. *Breast Cancer Res* **7**, 279–285.

[11] Zhu Q, Cronin EB, Currier AA, Vine HS, Huang M, Chen N, and Xu C (2005). Benign versus malignant breast masses: optical differentiation with US-guided optical imaging reconstruction. *Radiology* **237**, 57–66.

[12] Fournier LS, Vanel D, Athanasiou A, Gatzemeier W, Masuykov IV, Padhani AR, Dromain C, Galetti K, Sigal R, Costa A, et al (2009). Dynamic optical breast imaging: a novel technique to detect and characterize tumor vessels. *Eur J Radiol* **69**, 43–49.

[13] Ueda S, Nakamiya N, Matsuura K, Shigekawa T, Sano H, Hirokawa E, Shimada H, Suzuki H, Oda M, Yamashita Y, et al (2013). Optical imaging of tumor vascularity associated with proliferation and glucose metabolism in early breast cancer: clinical application of total hemoglobin measurements in the breast. *BMC Cancer* **13**, 514.

[14] Zhu Q, DeFusco PA, Ricci AJ, Cronin EB, Hegde PU, Kane M, Tavakoli B, Xu Y, Hart J, and Tannenbaum SH (2013). Breast cancer: assessing response to neoadjuvant chemotherapy by using US-guided near-infrared tomography. *Radiology* **266**, 433–442.

[15] Zhi W, Gu X, Qin J, Yin P, Sheng X, Gao SP, and Li Q (2012). Solid breast lesions: clinical experience with US-guided diffuse optical tomography combined with conventional US. *Radiology* **265**, 371–378.

[16] Choi JS, Kim MJ, Youk JH, Moon HJ, Suh HJ, and Kim EK (2013). US-guided optical tomography: correlation with clinicopathologic variables in breast cancer. *Ultrasound Med Biol* **39**, 233–240. https://doi.org/10.1016/j.ultrasmedbio.2012.09.014.

[17] Eisenhauer EA, Therasse P, Bogaerts J, Schwartz LH, Sargent D, Ford R, Dancey J, Arbuck S, Gwyther S, Mooney M, et al (2009). New response evaluation criteria in solid tumours: revised RECIST guideline (version 1.1). *Eur J Cancer* **45**, 228–247.

[18] Schaafsma BE, van de Giessen M, Charehbili A, Smit VT, Kroep JR, Lelieveldt BP, Liefers GJ, Chan A, Lowik CW, Dijkstra J, et al (2015). Optical mammography using diffuse optical spectroscopy for monitoring tumor response to neoadjuvant chemotherapy in women with locally advanced breast cancer. *Clin Cancer Res* **21**, 577–584.

[19] Jiang S, Pogue BW, Carpenter CM, Poplack SP, Wells WA, Kogel CA, Forero JA, Muffly LS, Schwartz GN, Paulsen KD, et al (2009). Evaluation of breast tumor response to neoadjuvant chemotherapy with tomographic diffuse optical spectroscopy: case studies of tumor region-of-interest changes. *Radiology* **252**, 551–560.

[20] Zhu Q, Hegde PU, Ricci AJ, Kane M, Cronin EB, Ardeshirpour Y, Xu C, Aguirre A, Kurtzman SH, Deckers PJ, et al (2010). Early-stage invasive breast cancers: potential role of optical tomography with US localization in assisting diagnosis. *Radiology* **256**, 367–378.

[21] Cerussi A, Hsiang D, Shah N, Mehta R, Durkin A, Butler J, and Tromberg BJ (2007). Predicting response to breast cancer neoadjuvant chemotherapy using diffuse optical spectroscopy. *Proc Natl Acad Sci U S A* **104**, 4014–4019.

[22] Zhu Q, Tannenbaum S, Hegde P, Kane M, Xu C, and Kurtzman SH (2008). Noninvasive monitoring of breast cancer during neoadjuvant chemotherapy using optical tomography with ultrasound localization. *Neoplasia* **10**, 1028–1040 [PMCID:PMC2546597].

[23] Soliman H, Gunasekara A, Rycroft M, Zubovits J, Dent R, Spayne J, Yaffe MJ, and Czarnota GJ (2010). Functional imaging using diffuse optical spectroscopy of neoadjuvant chemotherapy response in women with locally advanced breast cancer. *Clin Cancer Res* **16**, 2605–2614.

[24] Jiang S, Pogue BW, Kaufman PA, Gui J, Jermyn M, Frazee TE, Poplack SP, DiFlorio-Alexander R, Wells WA, and Paulsen KD (2014). Predicting breast tumor response to neoadjuvant chemotherapy with diffuse optical spectroscopic tomography prior to treatment. *Clin Cancer Res* **20**, 6006–6015.

[25] Zhu Q, Wang L, Tannenbaum S, Ricci AJ, DeFusco P, and Hegde P (2014). Pathologic response prediction to neoadjuvant chemotherapy utilizing pretreatment near-infrared imaging parameters and tumor pathologic criteria. *Breast Cancer Res* **16**, 456. https://doi.org/10.1186/s13058-014-0456-0.

[26] Busch DR, Choe R, Rosen MA, Guo W, Durduran T, Feldman MD, Mies C, Czerniecki BJ, Tchou J, Demichele A, et al (2013). Optical malignancy parameters for monitoring progression of breast cancer neoadjuvant chemotherapy. *Biomed Opt Express* **4**, 105–121.

[27] Duffaud F and Therasse P (2000). New guidelines to evaluate the response to treatment in solid tumors. *Bull Cancer* **87**, 881–886 [PMID:11174117].

[28] *AIUM practice guideline for the performance of a breast ultrasound examinationJ Ultrasound Med* **28**, 105–109 [PMID:19106368].

[29] Ogston KN, Miller ID, Payne S, Hutcheon AW, Sarkar TK, Smith I, Schofield A, and Heys SD (2003). A new histological grading system to assess response of breast cancers to primary chemotherapy: prognostic significance and survival. *Breast* **12**, 320–327.

[30] An YY, Kim SH, Kang BJ, and Lee AW (2015). Treatment response evaluation of breast cancer after neoadjuvant chemotherapy and usefulness of the imaging parameters of MRI and PET/CT. *J Korean Med Sci* **30**, 808–815. https://doi.org/10.3346/jkms.2015.30.6.808.

[31] Pakalniskis MG, Wells WA, Schwab MC, Froehlich HM, Jiang S, Li Z, Tosteson TD, Poplack SP, Kaufman PA, Pogue BW, et al (2011). Tumor angiogenesis change estimated by using diffuse optical spectroscopic tomography: demonstrated correlation in women undergoing neoadjuvant chemotherapy for invasive breast cancer? *Radiology* **259**, 365–374.

[32] Roubidoux MA, LeCarpentier GL, Fowlkes JB, Bartz B, Pai D, Gordon SP, Schott AF, Johnson TD, and Carson PL (2005). Sonographic evaluation of early-stage breast cancers that undergo neoadjuvant chemotherapy. *J Ultrasound Med* **24**, 885–895.

[33] Kuo WH, Chen CN, Hsieh FJ, Shyu MK, Chang LY, Lee PH, Liu LY, Cheng CH, Wang J, and Chang KJ (2008). Vascularity change and tumor response to neoadjuvant chemotherapy for advanced breast cancer. *Ultrasound Med Biol* **34**, 857–866.

[34] Vander HM, Cantley LC, and Thompson CB (2009). Understanding the Warburg effect: the metabolic requirements of cell proliferation. *Science* **324**, 1029–1033. https://doi.org/10.1126/science.1160809.

[35] Schwarz-Dose J, Untch M, Tiling R, Sassen S, Mahner S, Kahlert S, Harbeck N, Lebeau A, Brenner W, Schwaiger M, et al (2009). Monitoring primary systemic therapy of large and locally advanced breast cancer by using sequential positron emission tomography imaging with [18F]fluorodeoxyglucose. *J Clin Oncol* **27**, 535–541.

[36] Rousseau C, Devillers A, Sagan C, Ferrer L, Bridji B, Campion L, Ricaud M, Bourbouloux E, Doutriaux I, Clouet M, et al (2006). Monitoring of early response to neoadjuvant chemotherapy in stage II and III breast cancer by [18F]fluorodeoxyglucose positron emission tomography. *J Clin Oncol* **24**, 5366–5372.

[37] Falou O, Soliman H, Sadeghi-Naini A, Iradji S, Lemon-Wong S, Zubovits J, Spayne J, Dent R, Trudeau M, Boileau JF, et al (2012). Diffuse optical spectroscopy evaluation of treatment response in women with locally advanced breast cancer receiving neoadjuvant chemotherapy. *Transl Oncol* **5**, 238–246.